nature astronomy

SUPPLEMENTARY INFORMATION
https://doi.org/10.1038/s41550-018-0551-8

In the format provided by the authors and unedited.

The inside-out planetary nebula around a born-again star

Martín A. Guerrero[1*], Xuan Fang[2], Marcelo M. Miller Bertolami[3,4], Gerardo Ramos-Larios[5], Helge Todt[6], Alexandre Alarie[7], Laurence Sabin[7], Luis F. Miranda[1], Christophe Morisset[7], Carolina Kehrig[1] and Saúl A. Zavala[8]

[1]Instituto de Astrofísica de Andalucía, IAA-CSIC, Granada, Spain. [2]Laboratory for Space Research & Department of Physics, Faculty of Science, The University of Hong Kong, Hong Kong, People's Republic of China. [3]Instituto de Astrofísica de La Plata, UNLP-CONICET, La Plata, Argentina. [4]Facultad de Ciencias Astronómicas y Geofísicas, UNLP, La Plata, Argentina. [5]Instituto de Astronomía y Meteorología, Departamento de Física CUCEI, Universidad de Guadalajara, Guadalajara, Jalisco, Mexico. [6]Institute of Physics and Astronomy, University of Potsdam, Potsdam, Germany. [7]Instituto de Astronomía, Universidad Nacional Autónoma de México, Ensenada, Baja California, Mexico. [8]Tecnológico Nacional de México/I.T. Ensenada, Departamento de Ciencias Básicas, Ensenada, Baja California, Mexico. *e-mail: mar@iaa.es

The inside-out planetary nebula around a [WC] star in the making

Supplementary Table 1.– Chemical abundances of IRAS 17514 and low-mass VLTP sequences.

Initial Mass	H	^{4}He	^{12}C	^{13}C	^{14}N	^{16}O	^{20}Ne	^{22}Ne
IRAS 17514	0.01–0.05	0.33±0.10	0.50±0.10		0.01	0.1	0.04	
0.8 $M_{\odot}$	0.030	0.52	0.30	0.041	0.016	0.086	9×10^{-5}	1×10^{-3}
0.9 $M_{\odot}$	5×10^{-3}	0.48	0.29	0.069	0.065	0.091	9×10^{-5}	9×10^{-4}
1.0 $M_{\odot}$	5×10^{-5}	0.40	0.34	0.074	0.056	0.116	9×10^{-4}	0.01
1.1 $M_{\odot}$	5×10^{-3}	0.38	0.37	0.059	0.028	0.145	9×10^{-4}	0.01
1.25 $M_{\odot}$	5×10^{-6}	0.41	0.33	0.067	0.047	0.133	9×10^{-4}	0.01

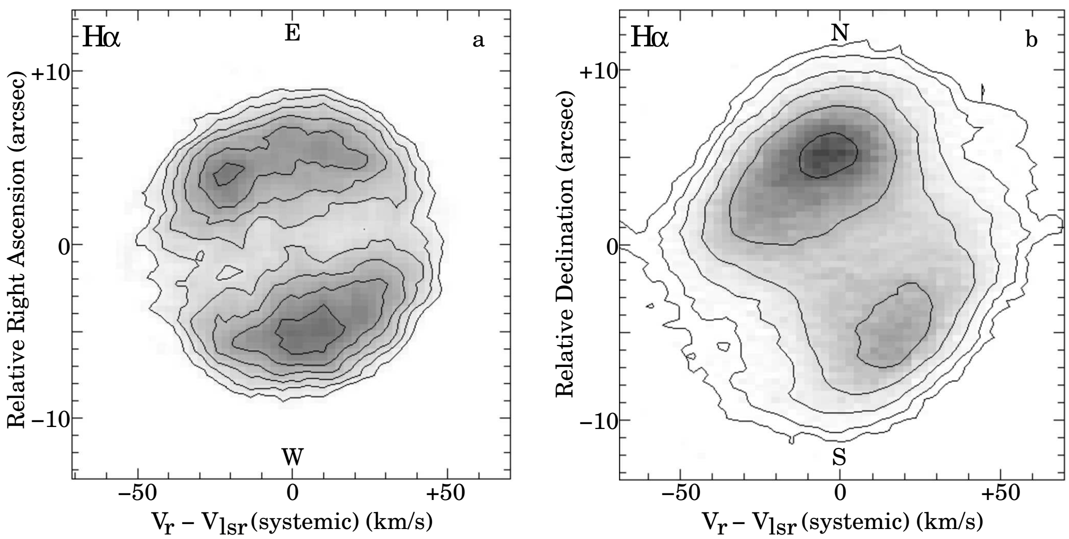

Supplementary Figure 1.– Position-velocity (PV) maps of the Hα emission line from the outer shell of HuBi 1 as observed through a long-slit placed on the CSPN at PA 90° (a) and PA 0° (b). The line intensity is shown in grey-scale and contours. The spatial origin corresponds to the position of the CSPN, whereas the radial velocities are relative to the systemic velocity of the nebula of +64.8 km s^{-1} as measured in the local standard of rest (LSR).

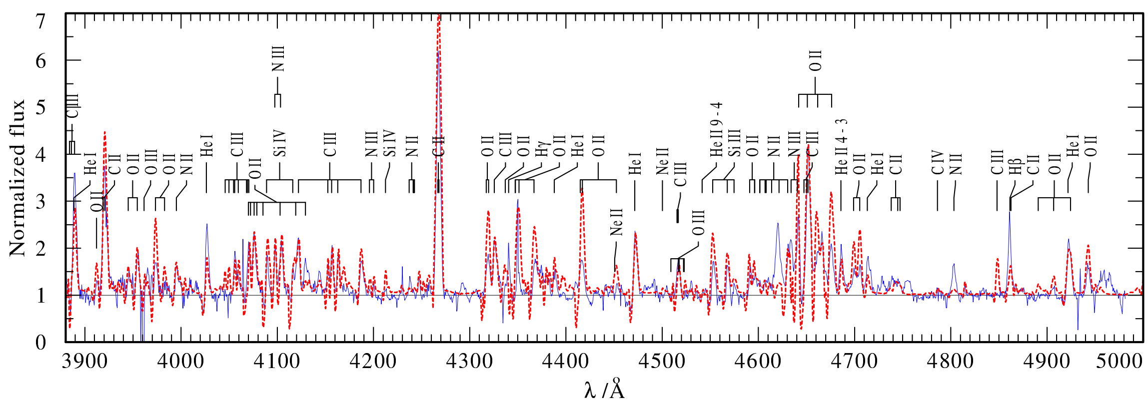

Supplementary Figure 2.– Optical spectrum of IRAS 17514 (blue) superimposed by the best-fit PoWR model (red). The identifications of key lines are labeled.

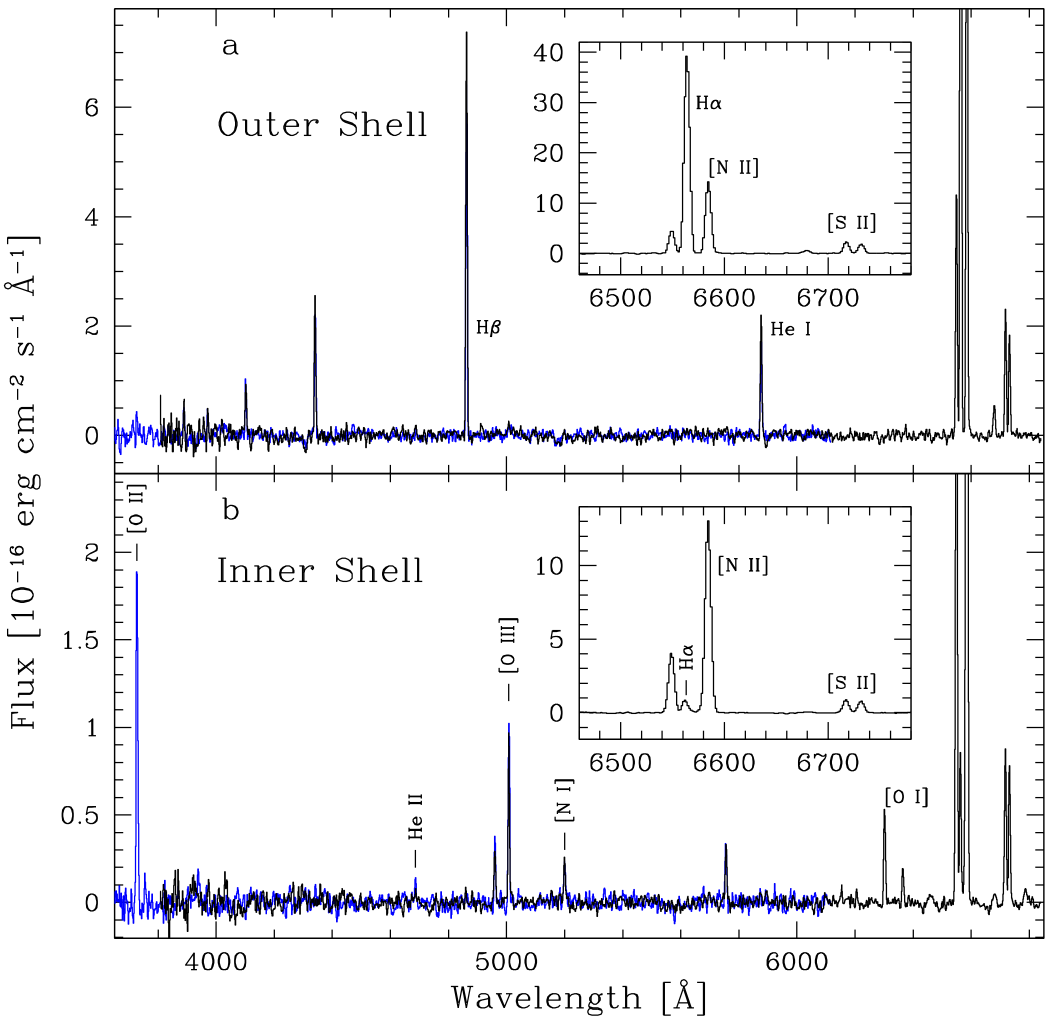

Supplementary Figure 3.– NOT ALFOSC grism #7 (black) and #14 (blue) spectra of the outer (a) and inner (b) shells of HuBi 1. The insets show the spectral range including the Hα, [N II] $\lambda\lambda$6548,6584, and [S II] $\lambda\lambda$6717,6731 emission lines. Note the singular detection of the He II λ4686 emission line in the inner shell.

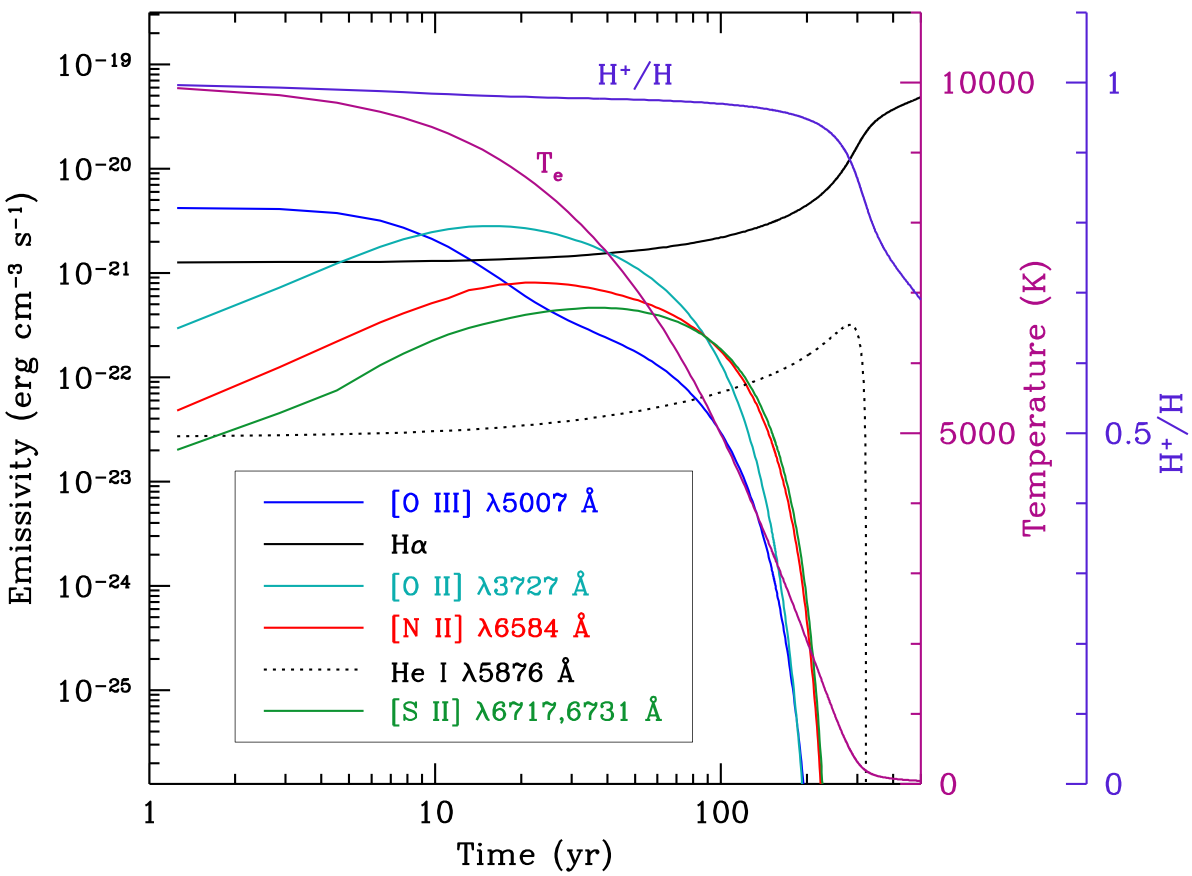

Supplementary Figure 4.– Time-evolution of the electron temperature T_e, hydrogen ionization fraction H^+/H, and emissivity of the Hβ, He I λ5876, [O II] λ3727, [O III] λ5007, [N II] λ6584, and [S II] $\lambda\lambda$6716,6731 emission lines of a photo-ionized cloud of gas with solar abundances, electron density of 200 cm^{-3} and electron temperature of 10,000 K after the ionizing source is switched off at time t=0.

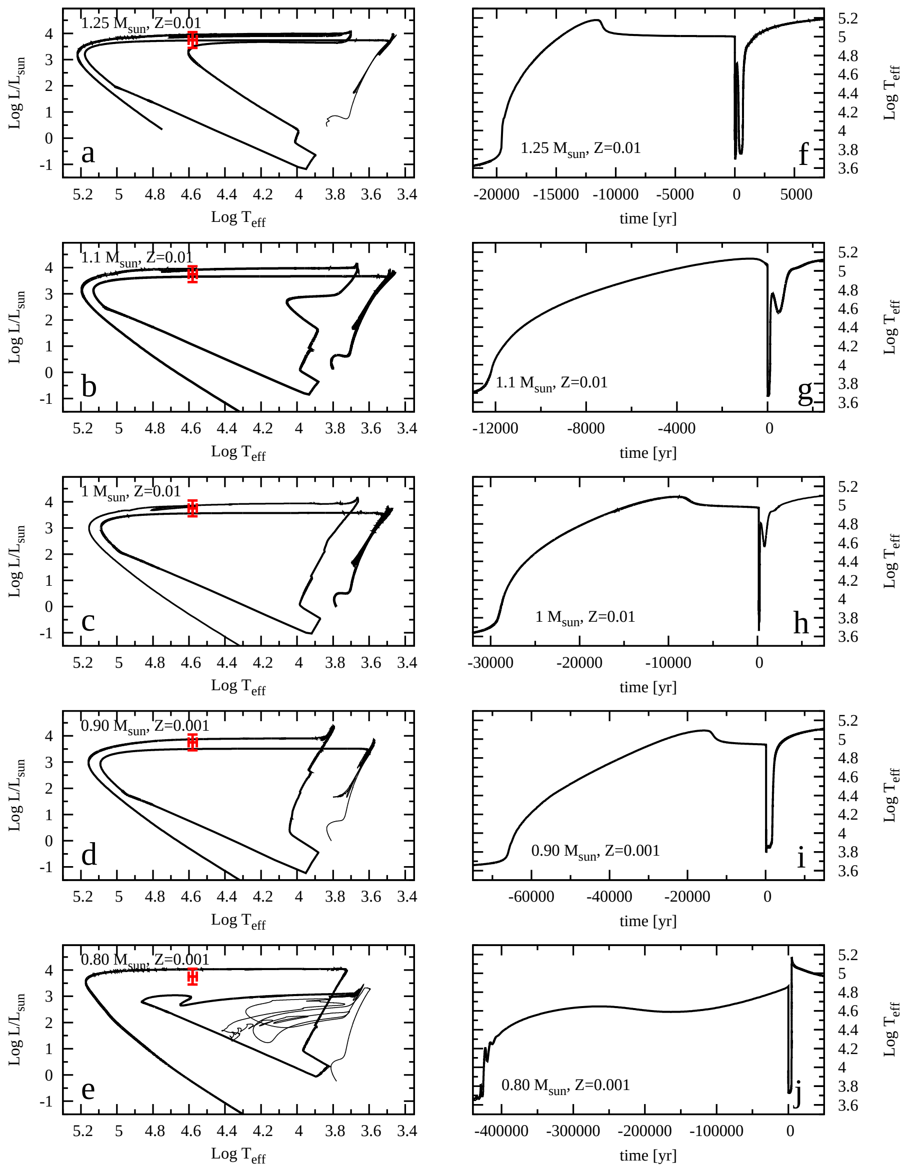

Supplementary Figure 5.– VLTP sequences of low-mass stars. (left) Evolution of the stellar sequences in the HR diagram, where the red-cross indicates the location of the central star of HuBi 1 with uncertainties as inferred from our best-fit non-LTE model (see the details of the non-LTE model fit). (right) Effective temperature evolution of the same sequences during the departure from the AGB and after the VLTP event (set at t=0).

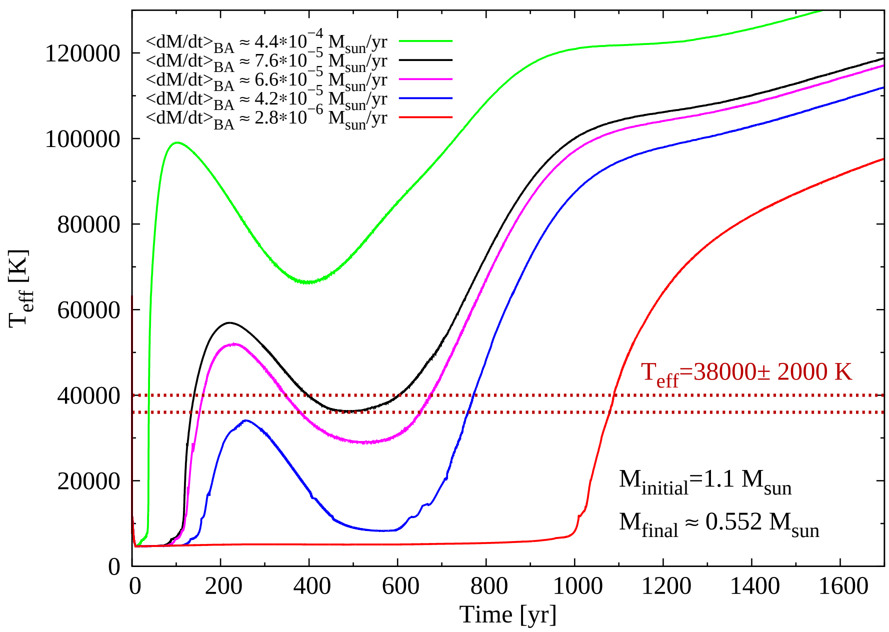

Supplementary Figure 6.– Predicted T_{eff} evolution of our 1.1 $M_{\odot}$ sequence after the VLTP event under different assumptions of the mass-loss rate through winds during the born-again AGB phase. The legend indicates the mean envelope mass removed per year at $\log T_{eff} < 3.8$.